Biotech Studies 33(1), xx-xx
http://doi.org/10.38042/

EARLY VIEW
RESEARCH PAPER

BIOTECH STUDIES

Barley preferentially activates strategy-II iron uptake mechanism under iron deficiency

Emre Aksoy[1]*

[1] Biological Sciences, Middle East Technical University, 06800 Ankara, Türkiye

Article History
Received 13 September 2023
Accepted 29 December 2023
First Online 08 February 2024

Corresponding Author
Tel.: +903122106464
E-mail: emreaks@metu.edu.tr

Keywords
Ferric chelate reductase activity
Gene expression
Iron deficiency
Phytosiderophore secretion
Rhizosphere acidification

Abstract

Plants utilize two main strategies for iron (Fe) uptake from the rhizosphere. Strategy-I is based on the reduction of ferric (Fe^{3+}) to ferrous (Fe^{2+}) iron by ferric chelate reductase (FCR) and is mainly observed in dicots. Strategy-II utilizes the complexation of Fe^{3+} with phytosiderophores secreted from the plant roots and mainly evolved in Gramineous species, including barley (*Hordeum vulgare*). Recent studies suggest that some species use a combination of both strategies for more efficient Fe uptake. However, the preference of barley for these strategies is not well understood. This study investigated the physiological and biochemical responses of barley under iron deficiency and examined the expression levels of the genes involved in Strategy-I and Strategy-II mechanisms in the roots. Fe deficiency led to decreased root and shoot lengths, fresh and dry weights, and Fe accumulation in the roots. Parallel to the chlorosis observed in the leaves, FCR activity and rhizosphere acidification were also significantly reduced in the roots, while the release of phytosiderophores increased. Furthermore, Strategy-II genes expressed higher than the Strategy-I genes in the roots under Fe deficiency. These findings demonstrate that Strategy-II is more activated than Strategy-I for Fe uptake in barley roots under Fe-deficient conditions.

Introduction

Iron (Fe) is an important nutrient for plant growth and development because it functions as a cofactor for enzymes involved in important biochemical pathways such as DNA and chlorophyll biosynthesis. Fe deficiency leads to interveinal leaf chlorosis, a decrease in leaf and root biomasses, and yield losses (Nikolic & Pavlovic, 2018). Although iron is sufficiently found in the soil, plants cannot easily absorb it from the rhizosphere in the bioavailable form since it makes a complex with chelates easily in the soil (Lindsay & Schwab, 1982). This is a big problem, especially for crops grown in alkaline soils because the increase in soil pH decreases the solubility of iron.

Two different mechanisms are evolved in plants for the uptake of iron into the roots (Aksoy *et al.*, 2018).

Dicots such as *Arabidopsis thaliana* mainly use a mechanism based on the reduction of ferric iron (Fe^{3+}) to ferrous iron (Fe^{2+}) (Strategy-I). In this mechanism, local acidification is performed by first releasing protons into the rhizosphere by H^+-ATPase (AHA) transporters located in the root epidermis (Santi & Schmidt, 2009). Subsequently, Fe^{3+} is reduced to soluble Fe^{2+} by an oxidoreductase named ferric chelate reductase (FCR/FRO) (Jeong & Connolly, 2009). Finally, Fe^{2+} ions are taken into the root epidermis via a metal transporter called IRON-RE

GULATED TRANSPORTER1 (IRT1) (Connolly *et al.*, 2002). The genes involved in Strategy I are upregulated under iron deficiency (Kobayashi & Nishizawa, 2012). In addition to Fe^{2+}, IRT1 can transport other divalent metals, including zinc (Zn^{2+}) and manganese (Mn^{2+}), and their concentrations increase dramatically in roots and shoots when plants are exposed to Fe deficiency (Vert *et al.*, 2002).

Gramineous plants such as barley (*Hordeum vulgare*) mainly use a chelation-based mechanism (Strategy-II) (Martín-Barranco *et al.*, 2021). Within this mechanism, plants produce various phytosiderophores (PS) through the sulfur assimilation pathway. In PS production, firstly S-adenosyl-L-methionine (SAM) is converted to nicotianamine (NA) by NICOTIANAMINE SYNTHASE (NAS), then NA is converted to 3'-keto acid by NICOTIANAMINE AMINOTRANSPHERESE (NAAT), and finally, 3'-keto acid is converted to 2'-deoxymugineic acid (DMA) by DEOXYMUGINEIC ACID SYNTHASE (DMAS). DMA is converted to mugineic acid (MA) by IRON DEFICIENCY SPECIFIC CLONE3 (IDS3), which functions as a dioxygenase in barley roots (Kobayashi *et al.*, 2001). Nine MAs have been identified so far in rye and barley (Bandyopadhyay & Prasad, 2021). They are released from plant roots to the rhizosphere as PS via TRANSPORTER OF MA1 (TOM1) (Nozoye *et al.*, 2011), forming a complex with insoluble Fe^{3+} in the soil, and then they are taken up into the root epidermis by specific oligopeptide transporters such as YELLOW STRIPE1 (YS1) in *Zea mays* and YELLOW STRIPE-LIKE15 (YSL15) in *Oryza sativa* (Aksoy *et al.*, 2018; Rai *et al.*, 2021). Similar to IRT1 in nongraminaceous plants, *Z. mays* YS1 serves as a major entry point for metals, utilizing the PS precursor NA to transport both beneficial (Fe^{2+}) and potentially hazardous (Fe^{3+}, Zn^{2+}, Mn^{2+}) ions into the plant (Murata *et al.*, 2006).

Previous studies showed that *O. sativa IRT1* and *IRT2* were induced in the roots under Fe deficiency (Ishimaru *et al.*, 2006; Walker & Connolly, 2008). Similar results were also shown in *Z. mays*, where *IRT1* and *IRT2* were upregulated by Fe deficiency in the roots (Li *et al.*, 2013; Li *et al.*, 2022), and *Triticum aestivum*, where *FRO2-2A* and *IRT1a-4A* were highly upregulated under Fe deficiency (Hua *et al.*, 2022). Opposite to these results, the expression of *ZmIRT1, Sorghum bicolor IRT1* and *Triticum polonicum IRT1A,* and *IRT1B* were not altered by Fe deficiency in maize (Wairich *et al.*, 2019), sorghum (Wairich *et al.*, 2019) and wheat (Jiang *et al.*, 2021), respectively. The inconsistent upregulation of *IRT* transporters across Gramineae suggests a fundamental ambiguity: is Strategy-I truly ubiquitous within this clade, or does its deployment remain an enigmatic, species-dependent phenomenon? To unravel this ambiguity in barley (*Hordeum vulgare* L.), a comprehensive approach was employed, examining the physiological, biochemical, and molecular aspects of barley under Fe deficiency, focusing specifically on transporter expression levels. This study was designed to elucidate whether barley utilizes both Strategy-I and Strategy-II, or exhibits a species-specific reliance on one strategy over the other.

Material &Methods

Plant material

Seeds of the Turkish barley cultivar Tarm-92 were obtained from the Bahri Dağdaş International Agricultural Research Institute, Turkey. Developed in 1992 by the Field Crops Central Research Institute, Tarm-92 is a medium-early barley cultivar with high tillering capacity, resistance to lodging, drought, salinity, and high temperature (Benlioğlu, B., & Özkan, 2015; Doğru *et al.*, 2020). While sensitive to lead and selenium (Doğru, 2019; Çakır, 2007), it exhibits tolerance to boron toxicity (Torun *et al.*, 2002; Öz, 2012; Çatav *et al.*, 2023) and Zn deficiency (Erenoglu *et al.*, 2000). Despite sensitivity to Fe deficiency (Erenoglu *et al.*, 2000), Tarm-92's molecular responses under this stress were unstudied, leaving its preferred Fe uptake strategy from the rhizosphere unknown.

Plant growth and stress application

For surface sterilization, barley seeds were shaken in a solution containing 3% sodium hypochlorite (Sigma) and 0.05% Tween-20 (Sigma) for 20 minutes and were washed five times with sterile distilled water. For germination, the seeds were placed in plastic Petri dishes containing sterile filter papers moistened with 3 mL of half-strength (1/2) Hoagland's nutrient solution (Hoagland & Arnon, 1950) at 22 ± 2 °C in a growth chamber for 2 days in the dark under 70% relative humidity. While preserving root integrity, the pre-germinated seedlings were meticulously positioned through a cheesecloth membrane atop 150 mL plastic containers (diameter: 10 cm) containing 1/2 Hoagland's nutrient solution (pH 5.8) supplemented with 50 µM Fe^{3+}-EDTA (Sigma) sufficient for barley growth. The plants were grown in a growth chamber at 22 ± 2 °C for 7 days under 70% relative humidity, on a 16-hour light (300 µmol m^{-2} s^{-1}) and 8-hour dark cycle. The nutrient solution was regularly renewed every 24 hours to maintain consistent nutrient availability and prevent oxygen depletion. The experiment was carried out in 6 repetitions (plastic containers) according to the randomized block design, where 5 plants were grown in each container. Container positions were randomized daily using a random number generator to minimize environmental effects and maintain consistent growth conditions.

Stress treatment was carried out 7 days after the plants were transferred to the containers. For iron deficiency, Fe^{3+}-EDTA was not added to the nutrient solution; instead, a Fe chelator, 300 µM FerroZine (3-(2-Pyridyl)-5,6-diphenyl-1,2,4-triazine-p,p'-disulfonic acid monosodium salt hydrate - Sigma), was added to remove all potential iron from the nutrient solution (Aksoy *et al.*, 2013). Control groups were grown in fresh nutrient solution containing 50 µM Fe^{3+}-EDTA. On the fifth day following the stress application, relevant physiological, biochemical, and molecular analyses were performed on barley seedlings.

Physiological measurements

Following the stress application, the root and shoot lengths of the plants were measured with the help of a ruler and recorded. Measurements were made with a

total of thirty plants in six containers for each of the Fe-sufficient (control) and Fe-deficient (stress) media. Chlorophyll index was determined by the Soil Plant Analysis Development (SPAD) measurements (SPAD-502 Plus, Konica Minolta, Japan) from the first fully developed leaves. Next, the roots and shoots of the plants were separated, their length was measured with a ruler and their fresh weights were recorded. Then, the tissues were dried in an oven at 65 °C for 24 hours and their dry weights were recorded. All physiological and biochemical analyses were made with 15 plants in three containers for each Fe-sufficient and Fe-deficient media except for the length measurements, which were taken from 30 plants, and divalent metal concentrations, which were taken from 3 randomly selected plants.

Total chlorophyll content

Total chlorophyll content was determined from 100 mg of first fully developed leaves following extraction in 2 mL of 80% acetone using a plastic pestle in microcentrifuge tubes (Aksoy *et al.*, 2013). Samples were incubated in the extraction buffer for 24 hours in the dark at 4 °C for complete extraction. The absorbance readings of the extracts were determined at 470, 646.8, and 663.2 nm as compared to 80% acetone and the total chlorophyll content was calculated according to Lichtenthaler & Wellburn (1983).

FCR enzyme activity

For the measurement of FCR activity, first the root fresh weights were recorded after brief drying with tissue paper. Then, the root samples were incubated in a 20 mL of solution of 0.1 mM Fe (III)-EDTA (Sigma) and 0.3 mM ferrozine (Sigma) for 24 hours in the dark at room temperature (Aksoy & Koiwa, 2013). Then, the absorbance of the solution was read at 562 nm against the blank without roots. The enzyme activity was calculated with a molar extinction coefficient of 28.6 mM^{-1} cm^{-1}.

Phytosiderophore release

Phytosiderophore release was quantified according to Reichman & Parker (2007). Briefly, two hours after the lights are turned on, plant roots were washed with distilled water three times and transferred into 20 mL of 200 µM $CaCl_2$ to collect the exudates by incubating them in the growth chamber for 6 hours. Microbial degradation of the PS was inhibited by addition of 50 µg/L Micropur into the extraction solution. At the end of the incubation, exudates were filtered through a 0.45 µm filter and quantified by Fe-binding assay. 0.5 mL of 0.2 mM FeCl3 was added onto 10 mL filtered exudate solution and mixed for 15 minutes on a rotary shaker. Then, 1 mL of 1 M sodium acetate (pH 7.0) buffer is added into the mixture and it was shaken for another 10 minutes. The mixture was filtered into 0.25 mL of 6 M HCl via a coarse filter paper to reduce Fe^{3+} to Fe^{2+} and 0.5 mL of 80 g/L hydroxylamine hydrochloride was added on top. Finally, the solution was incubated at 55°C for 30 minutes to complete the reduction process. When the solution was cooled down to room temperature, 0.25 mL of 2.5 g/L ferrozine and 1 mL of 2 M sodium acetate (pH 4.7) buffer were added to start the Fe-binding reaction. Immediately, the mixture was briefly mixed by hand and the absorbance was measured at 562 nm against the blank without plants. PS concentration was calculated according to standard curve generated by $FeCl_3$ series.

Divalent metal concentrations

For the measurement of root and leaf Fe, Zn, and Mn concentrations, the samples were incubated in 2 mM $CaSO_4$ and 10 mM EDTA for 10 minutes followed by washing twice with distilled water to eliminate any metal particles attached to the sample surface. Then, the samples were divided into 3 technical repeats of 100 mg and dried in test tubes for 24 hours at 65 °C (Aksoy *et al.*, 2013). Then, the samples were digested in 4 mL of 98.8% HNO_3 (Sigma) and 1 mL of concentrated HCl (Sigma) at 100 °C for 1 hour, 150 °C for 1 hour, 180 °C for 1.5 hours, and lastly at 210 °C until no liquid is left in the test tubes by using a furnace (Vasconcelos *et al.*, 2006). Finally, the samples were re-dissolved with 10 mL of 2% HNO_3, and the metal contents were determined in Inductively Coupled Plasma Mass Spectrometry (ICP-MS) (Bruker Aurora M90) in the pulse detector mode.

Rhizosphere acidification

The protons released from the roots were measured according to Pizzio *et al.* (2015) with minor modifications. Briefly, after the stress application, all plant roots were immersed in 20 mL of acidification solution (1/2 Hoagland's solution, 2 mM MES buffer, pH 5.8) and allowed to grow in the growth cabinet for an additional 48 hours. At the end of the incubation, the pH of the solution was measured with a pH meter (pH1000L, VWR) against the solution without plants. Then, the fresh weights of the plant roots were recorded. The pH = - log $[H^+]$ formula was used to calculate the proton release, according to the change in pH between the first and last reading.

Gene expression analyses by real-time PCR (RT-qPCR)

Total RNA was isolated from barley roots by RNeasy Plant Mini Kit (Qiagen). Genomic DNA contamination in the samples was removed using the RapidOut DNA Cleaning Kit (ThermoFisher). 1st strand cDNA synthesis from 2 µg of total RNA samples was performed using the RevertAid First Strand cDNA Synthesis Kit (ThermoFisher). 200 ng cDNA sample was amplified on a Rotorgene (Qiagen) with LightCycler 480 SYBR Green I Master Mix (Roche) in a total volume of 20 µL using 0.8 µM specific primers (Table 1). *HvACT* was used as a housekeeping gene in the normalization of gene expression (Gines *et al.* 2018). Gene expression analyses were performed two times (technical replicates) for each of the 3 biological replicates.

Statistical analyses

Differences between control and stress treatments were analyzed using the Minitab 19 package program according to Student's t-test (P<0.05).

Results & Discussion

Barley roots and shoots are adversely affected by Fe deficiency

Five days of Fe deficiency significantly impacted barley, highlighting its sensitivity to this nutrient limitation (Figure 1). Strikingly, root and shoot lengths plummeted significantly (P<0.05) by 40% and 20%, respectively (Figure 2a,b). This stunted growth extended to biomass, with 58.7% and 56.2% reductions in root and shoot fresh weights (Figure 2c,d) and 57.9% and 50.0% declines in dry weights (Figure 2e,f). Notably, Fe deficiency triggered visible chlorosis in leaves (Figure 3a), leading to a staggering 60.6% drop in total chlorophyll content compared to controls (Figure 3b). Chlorophyll index measurements confirmed this trend, revealing a 33.8% decrease under Fe deficiency (Figure 3c). This validates both measurements as reliable indicators of Fe deficiency-induced chlorophyll degradation in barley (Jiang *et al.*, 2017). Although a previous study reported more severe phenotypes under longer Fe deprivation (Erenoglu *et al.*, 2000), results of this current study demonstrate that just five days were sufficient to elicit clear deficiency symptoms in barley leaves. This aligns with research indicating a direct correlation between treatment duration and chlorosis severity in Fe-sensitive cultivars (Bandyopadhyay & Prasad, 2021; Martín-Barranco *et al.*, 2021). Thus, Tarm-92 emerges as highly sensitive to Fe deficiency, exhibiting significant impairments even after a short-term deprivation.

Fe accumulation in the roots and shoots of barley show opposite trends under Fe deficiency

Despite five days of Fe deficiency, shoot Fe concentrations remained remarkably stable (Figure 4). However, root Fe levels dropped by a significant 40.9% compared to controls (P<0.05). This selective decrease contradicts observations from longer-term studies where shoot Fe content fell substantially after comparable or even shorter Fe deprivations (Nikolic *et al.*, 2019; Mikami *et al.*, 2011; Erenoglu *et al.*, 2000). This divergence suggests two possibilities: either barley exhibits exceptional resilience in maintaining shoot Fe content even during short-term deficiency, or the five-day treatment window simply was not sufficient for significant depletion in shoots.

Intriguingly, the unchanged shoot Fe content did not prevent Fe deficiency responses. Both biomass and chlorophyll levels were markedly decreased (Figures 2 and 3), showcasing the plant's sensitivity despite seemingly adequate shoot Fe reserves. This raises the intriguing possibility that root Fe concentrations, despite their decline, trigger downstream signaling pathways in the leaves, activating deficiency responses even before impacting shoot iron stores. This hypothesis finds support in previous studies identifying root and leaf-derived signals under Fe deficiency (Hindt & Guerinot, 2012; Tabata, 2023). Alternatively, root Fe deprivation might trigger the overaccumulation of other divalent metals in leaves, reaching toxic levels and inducing chlorosis, as observed in some studies (Blasco *et al.*, 2018).

Fe deficiency causes overaccumulation of zinc and manganese in the roots and shoots of barley

Fe deficiency triggers the accumulation of other divalent metals, like Zn^{2+} and Mn^{2+}, which can be co-transported into the root epidermis by IRT1 (Connolly *et al.*, 2002) and YS1 (Murata *et al.*, 2006). As expected, barley plants exhibited significantly higher levels of these metals in both roots and shoots under Fe deficiency (Figure 5). Notably, Zn^{2+} concentrations in roots and shoots climbed a staggering 65.7% and 45.1%, respectively, while Mn^{2+} surged by a remarkable 209.1% and 43.7%. This striking overaccumulation suggests that IRT1 and/or YS1 overworks under Fe deficiency, inadvertently ushering in an influx of detrimental metals. Corroborating these findings, studies on tobacco (Kobayashi *et al.*, 2003) and maize (Mozafar, 1997; Kanai *et al.*, 2009) demonstrated similar Zn^{2+} and Mn^{2+} overaccumulation in roots and leaves under Fe deficiency, leading to impaired photosynthesis and biomass. Interestingly, other divalent metals, such as copper (Cu^{2+}) and cobalt (Co^{2+}) did not overaccumulate under Fe deficiency in tobacco (Kobayashi *et al.*, 2003) whereas Cu^{2+} concentration was increased in Arabidopsis leaves and roots (Vert *et al.*, 2002) and barley xylem (Alam *et al.*, 2001) under Fe deficiency. These data paint a concerning picture, where barley's observed chlorosis under Fe deficiency (significantly decreased chlorophyll content) might be driven not just by Fe scarcity, but also by a cascade of toxicity resulting from excessive Zn^{2+} and Mn^{2+} accumulation facilitated by IRT1 and/or YS1 (Panda *et al.*, 2012). Indeed, some studies provided evidence for the accumulation of reactive oxygen species (ROS) under Fe deficiency due to excessive Zn^{2+} and Mn^{2+} accumulation, preventing chlorophyll biosynthesis and active photosynthesis (Blasco *et al.*, 2018; Fan *et al.*, 2021). Without neglecting the direct effects of Fe deficiency on ROS production (Santos *et al.*, 2019), this highlights the intricate interplay between nutrient deficiencies and metal uptake pathways, urging further investigation into the specific mechanisms behind such collateral damage caused by Fe deficiency.

Strategy-I and Strategy-II are affected at the biochemical level in barley under Fe deficiency

To elucidate whether barley prioritizes the chelation-based Strategy-II or the reduction-based Strategy-I for Fe acquisition during deficiency, key biochemical parameters in the roots of barley were

investigated under Fe-limited conditions (Figure 6). Firstly, Strategy-II utilization was confirmed by quantifying the release of phytosiderophores (PS). As expected, barley unveiled its arsenal, raising PS levels a remarkable 4.2-fold under Fe deficiency compared to Fe sufficient condition (Figure 6a). This robust response aligns with previous reports highlighting a positive correlation between PS release rate, Fe deficiency tolerance, and treatment duration in barley (Erenoglu *et al.*, 2000; Rai *et al.*, 2021). Thus, barley appears to adhere to the canonical tenets of Strategy-II Fe acquisition. However, a striking incongruity emerged. Despite significantly elevated PS released from the roots, barley displayed pronounced symptoms of Fe deficiency, exemplified by higher chlorosis and reduced root Fe content. This dissociation between robust PS production and impaired Fe uptake suggests the possibility of an alternative, strategy employed by barley to compensate for the reduced efficiency of its Strategy-II system within the roots.

Following confirmation of Strategy-II utilization through elevated PS release, barley's Fe acquisition repertoire was further explored by examining the potential contribution of a complementary Strategy-I pathway. Intriguingly, we observed a significant reduction of traits associated with this pathway. FCR activity exhibited a substantial reduction of 47.9% under Fe deficiency (Figure 6b), while rhizosphere acidification, characterized by H^+ release, declined by 42.1% (Figure 6c). This deviation from the classic Strategy-I response, characterized by increased FCR activity and proton release (Aksoy *et al.*, 2018), suggests that barley does not readily engage this pathway to compensate for its apparent limitation in Strategy-II efficiency. While the observed reduction of Strategy-I in barley deviates from typical responses documented in non-Gramineae species, it highlights the intricate nature of plant Fe acquisition and the potential for species-specific adaptations. Some studies report enhanced FCR activity and rhizosphere acidification in Fe-tolerant non-Gramineae (Vasconcelos & Grusak, 2014), showcasing the diverse array of responses across plant lineages. Further complicating the picture, differences in timing and magnitude of these responses are apparent in diverse species. For instance, while FCR peaks in cucumber after five days of Fe deficiency (Pavlovic *et al.*, 2013) and Arabidopsis after 72 hours (Aksoy *et al.*, 2013), our barley model exhibited a significant decline in both FCR activity and rhizosphere acidification. Yet, interestingly, Mikami *et al.* (2011) reported a similar non-significant decrease in FCR activity in barley after seven days, suggesting potential intraspecific diversity in strategy utilization. Taken together, these data suggest that barley does not solely depend on Strategy-I to support the Strategy-II to uptake Fe from the rhizosphere, which means that it can utilize another alternative strategy to uptake Fe efficiently. Recently, an alternative Fe acquisition strategy was identified in non-Gramineae species (Robe *et al.*, 2021). In this strategy, plants secrete secondary metabolites like coumarins into the rhizosphere, which complexes with Fe^{3+}. Although, in silico evidence suggest that this strategy was not evolved in barley (Clemens & Weber, 2016), coumarin accumulation was shown in the vacuoles of barley leaf mesophyll cells (Werner & Matile, 1985).

This intricate tapestry of response patterns underscores the need for comparative studies across diverse plant models employing different Fe uptake strategies. By investigating a broader range of species and treatment timeframes, we can begin to elucidate the spectrum of adaptive plasticity in Fe acquisition and unravel the factors influencing specific pathway preferences. Such comprehensive research promises to advance our understanding of plant resilience and adaptability in the face of nutrient limitations.

The expression levels of genes responsible for Fe uptake are altered significantly in the roots of barley under Fe deficiency

The effect of short-term Fe deficiency on decreased root Fe levels but stable shoot Fe levels implies that the stress signaling was not sufficiently affected and the Fe translocation has not yet been altered in the early days of stress treatment in barley. To evaluate how stress signaling was affected in barley cultivar, the expression levels of the genes involved in both strategies were determined in the roots (Figure 7). Accordingly, the expression levels of *HvIRT1, HvIRT2, HvFRO1, HvFRO2,* and *HvAHA2* functioning in Strategy-I and *HvNAS1, HvIDS2, HvIDS3, HvYS1, HvTOM1* and *HvDMAS1* working in Strategy-II were increased significantly under Fe deficiency (Figure 7a). Similar to our results, the expression levels of the genes coding for IRT transporters (*IRT1* and *IRT2*), FCRs (*FRO1* and *FRO2*) and proton pump (*AHA2*) increases under Fe deficiency in non-Gramineous species (Hindt & Guerinot, 2012). Similarly, *HvIRT1* also increases in the roots of barley under Fe deficiency (Pedas *et al.*, 2008). The observed difference between FCR activity and rhizosphere acidification (Figure 6b and c) in relation to the expression levels of *HvFRO1, HvFRO2*, and *HvAHA2* suggests that, while the genes were activated after five days of iron deficiency, the corresponding enzymes may not have become fully functional. This aligns with the possibility that Strategy-II, as evidenced by PS release, is activated earlier for initial Fe acquisition, while Strategy-I may require a longer exposure to Fe deficiency to fully engage and support sufficient Fe uptake for tolerance. Further research investigating enzyme activity across longer timeframes may shed light on the activation dynamics of different Fe acquisition strategies in barley.

Among Strategy-II genes, *HvTOM1* and *HvIDS2* expressions increased by 10 folds while *HvNAS1* expression increased by 8.9 folds (Figure 7b). In a previous study, the expression levels of *HvDMAS1* and *HvNAS1* increased by four folds and the level of *HvTOM1* increased by three folds in barley roots under 7 days of Fe deficiency (Nikolic *et al.*, 2019). In the same study,

HvYS1 expression increased approximately 1.8 times in a 2-day stress application. In our study, genotypic and developmental stage differences may be among the reasons for the higher increases in the expression levels of the same genes in barley roots exposed to 5 days of Fe deficiency. Among Strategy-I genes, the top two genes with the highest expression levels were *HvAHA2* and *HvIRT1*, with 5.7 and 5.0-fold increases, respectively. Therefore, it is noteworthy that among the increases in gene expressions, the expression levels of genes involved in Strategy-II were higher than those in Strategy-I. These results are in with PS release rates (Figure 6a), suggesting that Strategy-II is the main Fe acquisition mechanism in barley roots.

Even though two Fe uptake strategies, namely Strategy-I and Strategy-II, were evolved in different plant groups, a combined strategy was proposed only for the cultivated rice to absorb Fe from the rhizosphere since it is adapted to live in paddies (Sperotto *et al.*, 2012), where Fe^{2+} is the more abundant form compared to Fe^{3+} in submerged conditions (Ishimaru *et al.*, 2006). Recently, this combined strategy was also shown in *Oryza* genus (Wairich *et al.*, 2019) and other Gramineous species, suggesting that plants have evolved alternative mechanisms to adapt to changing environmental conditions, such as flooding, to continue absorbing Fe from the rhizosphere. However, depending on the species, either one or both of the Fe uptake strategies may have been selectively employed for efficient Fe acquisition (Grillet, & Schmidt, 2019). Results presented in this study suggest that, while barley primarily relies on Strategy-II for Fe uptake evidenced by the substantial increase in PS levels (Figure 6a), this reliance should not mask the potential contribution of other mechanisms. The observed downregulation of Strategy-I components, like FCR activity and rhizosphere acidification, hints at potential limitations in solely relying on Strategy-II. Therefore, while Strategy-II appears to be the main player, alternative Fe uptake pathways, including components of Strategy-I, likely play a complementary role in supporting Fe acquisition in barley roots.

Conclusions

This study showed that the FCR activity and rhizosphere acidification, which take part in Strategy-I, decreased significantly in barley roots under iron deficiency. The decrease in both activities led to a reduction in the Fe accumulation in the roots. On the other hand, although no significant change was observed in the shoot Fe levels, the severity of the chlorosis in the leaves increased, which might be attributed to the over-accumulation of Zn and Mn. Plants secreted more phytosiderophores to the rhizosphere as a response to the Fe deficiency. The expression levels of genes involved in both Strategy-I and Strategy-II increased in the roots of barley exposed to iron deficiency, but this increase was more significant in Strategy-II genes. Taken together, the results of this study prove that the Tarm-92 is sensitive to Fe deficiency and it activates Strategy-II stronger than Strategy-I under Fe deficiency.

Funding Information

This study was supported by the Niğde Ömer Halisdemir University Research Projects Unit (project number GTB 2017/01-BAGEP) and the COST Association (grant CA19116 “PLANTMETALS”).

References

Aksoy, E., Jeong, I. S., & Koiwa, H. (2013). Loss of function of Arabidopsis C-terminal domain phosphatase-like1 activates iron deficiency responses at the transcriptional level. *Plant Physiology*, *161*(1), 330-345. https://doi.org/10.1104/pp.112.207043

Aksoy, E., & Koiwa, H. (2013). Determination of ferric chelate reductase activity in the *Arabidopsis thaliana* root. *Bio-protocol*, *3*(15), e843-e843. https://doi.org/10.21769/BioProtoc.843

Aksoy, E., Yerlikaya, B. A., Ayten, S., & Abudureyimu, B. (2018). Iron uptake mechanisms from the rhizosphere in plants. *Turkish Journal of Agriculture-Food Science and Technology*, *6*(12), 1673-1683. https://doi.org/10.24925/turjaf.v6i12.1673-1683.1326

Alam, S., Kamei, S., & Kawai, S. (2001). Effect of iron deficiency on the chemical composition of the xylem sap of barley. *Soil Science and Plant Nutrition*, *47*(3), 643-649. https://doi.org/10.1080/00380768.2001.10408428

Bandyopadhyay, T., & Prasad, M. (2021). IRONing out stress problems in crops: a homeostatic perspective. *Physiologia Plantarum*, *171*(4), 559-577. https://doi.org/10.1111/ppl.13184

Benlioğlu, B., & Özkan, U. (2015). Bazı arpa çeşitlerinin (*Hordeum vulgare* L.) çimlenme dönemlerinde farklı dozlardaki tuz stresine tepkilerinin belirlenmesi. *Tarla Bitkileri Merkez Araştırma Enstitüsü Dergisi*, *24*(2), 109-114. https://doi.org/10.21566/tbmaed.07412

Blasco, B., Navarro-León, E., & Ruiz, J.M. (2018). Oxidative stress in relation with micronutrient deficiency or toxicity. In M. A. Hossain, T. Kamiya, D.J. Burritt, L-S. P. Tran, & T. Fujiwara (Eds.), *Plant micronutrient use efficiency* (pp. 181-194). Academic Press. https://doi.org/10.1016/B978-0-12-812104-7.00011-3

Clemens, S., & Weber, M. (2016). The essential role of coumarin secretion for Fe acquisition from alkaline soil. *Plant Signaling and Behavior, 11*(2), e1114197. https://doi.org/10.1080/15592324.2015.1114197

Connolly, E. L., Fett, J. P., & Guerinot, M. L. (2002). Expression of the *IRT1* metal transporter is controlled by metals at the levels of transcript and protein accumulation. *The Plant Cell*, *14*(6), 1347-1357. https://doi.org/10.1105/tpc.001263

Çakır S. (2007). Selenyum Toksisitesinin İki Arpa (*Hordeum vulgare* L.) Çeşitinde (TARM 92, BÜLBÜL 89) Antioksidan Enzim Aktivitesine Etkisi, Yüksek Lisans Tezi, Fen Bilimleri Enstitüsü, Erciyes Üniversitesi, Kayseri.

Çatav, Ş.S., Çetin, E., Vural, E., & Bürün, B. (2023). Boron toxicity tolerance in barley may be related to intrinsically higher levels of reactive oxygen species in the shoots. *Botanica Serbica*, *47*(1), 113-124.

https://doi.org/10.2298/BOTSERB2301113C

Doğru, A. (2019). Bazi arpa genotiplerinde kurşun toleransinin klorofil a floresansi ile değerlendirilmesi. *Bartın University International Journal of Natural and Applied Sciences*, *2*(2), 228-238.

Doğru, A., 2020. Evaluation of Heat Shock-Induced Stress Tolerance to Some Abiotic Factors in Barley Seedlings by Chlorophyll a Fluorescence Technique. *Sinop Üniversitesi Fen Bilimleri Dergisi*, *5*(2), 112-124. https://doi.org/10.33484/sinopfbd.630690

Erenoglu, B., Eker, S., Cakmak, I., Derici, R., & Römheld, V. (2000). Effect of iron and zinc deficiency on release of phytosiderophores in barley cultivars differing in zinc efficiency. *Journal of Plant Nutrition*, *23*(11-12), 1645-1656. https://doi.org/10.1080/01904160009382130

Fan, X., Zhou, X., Chen, H., Tang, M., & Xie, X. (2021). Cross-talks between macro-and micronutrient uptake and signaling in plants. *Frontiers in Plant Science*, *12*, 663477. https://doi.org/10.3389/fpls.2021.663477

Gines, M., Baldwin, T., Rashid, A., Bregitzer, P., Maughan, P. J., Jellen, E. N., & Klos, K. E. (2018). Selection of expression reference genes with demonstrated stability in barley among a diverse set of tissues and cultivars. *Crop Science*, *58*(1), 332-341. https://doi.org/10.2135/cropsci2017.07.0443

Grillet, L., & Schmidt, W. (2019). Iron acquisition strategies in land plants: not so different after all. *New Phytologist, 224*(1), 11-18. https://doi.org/10.1111/nph.16005

Hindt, M.N., & Guerinot, M.L. (2012). Getting a sense for signals: regulation of the plant iron deficiency response. *Biochimica et Biophysica Acta (BBA)-Molecular Cell Research*, *1823*(9), 1521-1530. https://doi.org/10.1016/j.bbamcr.2012.03.010

Hoagland, D. R., & Arnon, D. I. (1950). The water-culture method for growing plants without soil. *California Agricultural Experiment Station Circular*, *347*(2), 32.

Hua, Y. P., Wang, Y., Zhou, T., Huang, J. Y., & Yue, C. P. (2022). Combined morpho-physiological, ionomic and transcriptomic analyses reveal adaptive responses of allohexaploid wheat (*Triticum aestivum* L.) to iron deficiency. *BMC Plant Biology, 22*(1), 234. https://doi.org/10.1186/s12870-022-03627-4

Ishimaru, Y., Suzuki, M., Tsukamoto, T., Suzuki, K., Nakazono, M., Kobayashi, T., Wada, Y., Watanabe, S., Matsuhashi, S., Takahashi, M., & Nishizawa, N. K. (2006). Rice plants take up iron as an Fe^{3+}-phytosiderophore and as Fe^{2+}. *The Plant Journal, 45*(3), 335-346. https://doi.org/10.1111/j.1365-313X.2005.02624.x

Jiang, Y., Chen, X., Chai, S., Sheng, H., Sha, L., Fan, X., Zeng, J., Kang, H., Zhang, H., Xiao, X., & Zhou, Y. (2021). *TpIRT1* from Polish wheat (*Triticum polonicum* L.) enhances the accumulation of Fe, Mn, Co, and Cd in Arabidopsis. *Plant Science, 312,* 111058. https://doi.org/10.1016/j.plantsci.2021.111058

Jiang, C., Johkan, M., Hohjo, M., Tsukagoshi, S., & Maruo, T. (2017). A correlation analysis on chlorophyll content and SPAD value in tomato leaves. *HortResearch, 71*(71), 37-42.

Jeong, J., & Connolly, E. L. (2009). Iron uptake mechanisms in plants: functions of the FRO family of ferric reductases. *Plant science*, *176*(6), 709-714. https://doi.org/10.1016/j.plantsci.2009.02.011

Kanai, M., Hirai, M., Yoshiba, M., Tadano, T., & Higuchi, K. (2009). Iron deficiency causes zinc excess in *Zea mays*. *Soil Science and Plant Nutrition, 55*(2), 271-276. https://doi.org/10.1111/j.1747-0765.2008.00350.x

Kobayashi, T., & Nishizawa, N. K. (2012). Iron uptake, translocation, and regulation in higher plants. *Annual Review of Plant Biology*, *63*, 131-152. https://doi.org/10.1146/annurev-arplant-042811-105522

Kobayashi, T., Nakanishi, H., Takahashi, M., Kawasaki, S., Nishizawa, N.K., & Mori, S. (2001). In vivo evidence that *Ids3* from *Hordeum vulgare* encodes a dioxygenase that converts 2'-deoxymugineic acid to mugineic acid in transgenic rice. *Planta*, *212*, 864-871. https://doi.org/10.1007/s004250000453

Kobayashi, T., Yoshihara, T., Jiang, T., Goto, F., Nakanishi, H., Mori, S., & Nishizawa, N.K. (2003). Combined deficiency of iron and other divalent cations mitigates the symptoms of iron deficiency in tobacco plants. *Physiologia Plantarum, 119*(3), 400-408. https://doi.org/10.1034/j.1399-3054.2003.00126.x

Li, S., Song, Z., Liu, X., Zhou, X., Yang, W., Chen, J., & Chen, R. (2022). Mediation of zinc and iron accumulation in maize by ZmIRT2, a novel iron-regulated transporter. *Plant and Cell Physiology, 63*(4), 521-534. https://doi.org/10.1093/pcp/pcab177

Li, S., Zhou, X., Huang, Y., Zhu, L., Zhang, S., Zhao, Y., Guo, J., Chen, J., & Chen, R. (2013). Identification and characterization of the zinc-regulated transporters, iron-regulated transporter-like protein (ZIP) gene family in maize. *BMC Plant Biology, 13*(1), 1-14. https://doi.org/10.1186/1471-2229-13-114

Lichtenthaler, H. K., & Wellburn, A. R. (1983). Determinations of total carotenoids and chlorophylls a and b of leaf extracts in different solvents. *Biochemical Society Transactions, 11(5)*, 591–592. https://doi.org/10.1042/bst0110591

Lindsay, W. L., & Schwab, A. P. (1982). The chemistry of iron in soils and its availability to plants. *Journal of Plant Nutrition*, *5*(4-7), 821-840. https://doi.org/10.1080/01904168209363012

Martín-Barranco, A., Thomine, S., Vert, G., & Zelazny, E. (2021). A quick journey into the diversity of iron uptake strategies in photosynthetic organisms. *Plant Signaling and Behavior*, *16*(11), 1975088. https://doi.org/10.1080/15592324.2021.1975088

Mikami, Y., Saito, A., Miwa, E., & Higuchi, K. (2011). Allocation of Fe and ferric chelate reductase activities in mesophyll cells of barley and sorghum under Fe-deficient conditions. *Plant Physiology and Biochemistry*, *49*(5), 513-519. https://doi.org/10.1016/j.plaphy.2011.01.009

Mozafar, A. (1997). Distribution of nutrient elements along the maize leaf: Alteration by iron deficiency. *Journal of Plant Nutrition, 20*(7-8), 999-1005. https://doi.org/10.1080/01904169709365312

Murata, Y., Ma, J.F., Yamaji, N., Ueno, D., Nomoto, K., & Iwashita, T. (2006). A specific transporter for iron (III)–phytosiderophore in barley roots. *The Plant Journal, 46*(4), 563-572. https://doi.org/10.1111/j.1365-313X.2006.02714.x

Nikolic, D.B., Nesic, S., Bosnic, D., Kostic, L., Nikolic, M. & Samardzic, J.T. (2019). Silicon alleviates iron

deficiency in barley by enhancing expression of strategy II genes and metal redistribution. *Frontiers in Plant Science, 10*, 416. https://doi.org/10.3389/fpls.2019.00416

Nikolic, M. & Pavlovic, J. (2018). Plant responses to iron deficiency and toxicity and iron use efficiency in plants. Oxidative stress in relation with micronutrient deficiency or toxicity. In M. A. Hossain, T. Kamiya, D.J. Burritt, L-S. P. Tran, & T. Fujiwara (Eds.), *Plant micronutrient use efficiency* (pp. 55-69). Academic Press. https://doi.org/10.1016/B978-0-12-812104-7.00004-6

Nozoye, T., Nagasaka, S., Kobayashi, T., Takahashi, M., Sato, Y., Sato, Y., Uozumi, N., Nakanishi, H. & Nishizawa, N.K. (2011). Phytosiderophore efflux transporters are crucial for iron acquisition in graminaceous plants. *Journal of Biological Chemistry*, *286*(7), 5446-5454. https://doi.org/10.1074/jbc.M110.180026

Öz M. T. (2012). Microarray based expression profiling of barley under boron stress and cloning of 3H boron tolerance gene. PhD Thesis, Middle East Technical University, Ankara, Türkiye.

Panda, B. B., Sharma, S. G., Mohapatra, P. K., & Das, A. (2012). Iron stress induces primary and secondary micronutrient stresses in high yielding tropical rice. *Journal of Plant Nutrition*, *35*(9), 1359-1373. https://doi.org/10.1080/01904167.2012.684128

Pavlovic, J., Samardzic, J., Maksimović, V., Timotijevic, G., Stevic, N., Laursen, K.H., Hansen, T.H., Husted, S., Schjoerring, J.K., Liang, Y., & Nikolic, M. (2013). Silicon alleviates iron deficiency in cucumber by promoting mobilization of iron in the root apoplast. *New Phytologist*, *198*(4), 1096-1107. https://doi.org/10.1111/nph.12213

Pedas, P., Ytting, C.K., Fuglsang, A.T., Jahn, T.P., Schjoerring, J.K., & Husted, S. (2008). Manganese efficiency in barley: identification and characterization of the metal ion transporter HvIRT1. *Plant Physiology, 148*(1), 455-466. https://doi.org/10.1104/pp.108.118851

Pizzio, G. A., Regmi, K., & Gaxiola, R. (2015). Rhizosphere acidification assay. *Bio-protocol*, *5*(23), e1676-e1676. https://doi.org/10.21769/BioProtoc.1676

Rai, S., Singh, P.K., Mankotia, S., Swain, J., & Satbhai, S.B. (2021). Iron homeostasis in plants and its crosstalk with copper, zinc, and manganese. *Plant Stress, 1*, 100008. https://doi.org/10.1016/j.stress.2021.100008

Reichman, S. M., & Parker, D. R. (2007). Critical evaluation of three indirect assays for quantifying phytosiderophores released by the roots of Poaceae. *European Journal of Soil Science*, *58*(3), 844-853. https://doi.org/10.1111/j.1365-2389.2006.00874.x

Robe, K., Izquierdo, E., Vignols, F., Rouached, H., & Dubos, C. (2021). The coumarins: secondary metabolites playing a primary role in plant nutrition and health. *Trends in Plant Science, 26*(3), 248-259. https://doi.org/10.1016/j.tplants.2020.10.008

Santi, S., & Schmidt, W. (2009). Dissecting iron deficiency-induced proton extrusion in Arabidopsis roots. *New Phytologist*, *183*(4), 1072-1084. https://doi.org/10.1111/j.1469-8137.2009.02908.x

Santos, C.S., Ozgur, R., Uzilday, B., Turkan, I., Roriz, M., Rangel, A.O., Carvalho, S.M., & Vasconcelos, M.W. (2019). Understanding the role of the antioxidant system and the tetrapyrrole cycle in iron deficiency chlorosis. *Plants, 8*(9), 348. https://doi.org/10.3390/plants8090348

Sperotto, R. A., Ricachenevsky, F. K., de Abreu Waldow, V., & Fett, J. P. (2012). Iron biofortification in rice: it's a long way to the top. *Plant Science, 190*, 24-39. https://doi.org/10.1016/j.plantsci.2012.03.004

Tabata, R. (2023). Regulation of the iron-deficiency response by IMA/FEP peptide. *Frontiers in Plant Science, 14*, 1107405. https://doi.org/10.3389/fpls.2023.1107405

Torun, B., Kalayci, M., Ozturk, L., Torun, A., Aydin, M., & Cakmak, I. (2002). Differences in Shoot Boron Concentrations, Leaf Symptoms, and Yield of Turkish Barley Cultivars Grown on Boron-Toxic Soil in Field. *Journal of Plant Nutrition*, *26*(9), 1735-1747. https://doi.org/10.1081/PLN-120023279

Vasconcelos, M. W., & Grusak, M. A. (2014). Morpho-physiological parameters affecting iron deficiency chlorosis in soybean (*Glycine max* L.). *Plant and soil*, *374*, 161-172. https://doi.org/10.1007/s11104-013-1842-6

Vasconcelos, M., Eckert, H., Arahana, V., Graef, G., Grusak, M.A., & Clemente, T. (2006). Molecular and phenotypic characterization of transgenic soybean expressing the Arabidopsis ferric chelate reductase gene, *FRO2*. *Planta, 224*, 1116-1128. https://doi.org/10.1007/s00425-006-0293-1

Vert, G., Grotz, N., Dédaldéchamp, F., Gaymard, F., Guerinot, M.L., Briat, J.F., & Curie, C. (2002). IRT1, an Arabidopsis transporter essential for iron uptake from the soil and for plant growth. *The Plant Cell*, *14*(6), 1223-1233. https://doi.org/10.1105/tpc.001388

Wairich, A., de Oliveira, B. H. N., Arend, E. B., Duarte, G. L., Ponte, L. R., Sperotto, R. A., Ricachenevsky, F.K., & Fett, J. P. (2019). The combined strategy for iron uptake is not exclusive to domesticated rice (*Oryza sativa*). *Scientific Reports, 9*(1), 16144. https://doi.org/10.1038/s41598-019-52502-0

Walker, E. L., & Connolly, E. L. (2008). Time to pump iron: iron-deficiency-signaling mechanisms of higher plants. *Current Opinion in Plant Biology, 11*(5), 530-535. https://doi.org/10.1016/j.pbi.2008.06.013

Werner, C., & Matile, P. (1985). Accumulation of coumarylglucosides in vacuoles of barley mesophyll protoplasts. *Journal of Plant Physiology, 118*(3), 237-249. https://doi.org/10.1016/S0176-1617(85)80225-X

Figure 1. Overall look of the barley plants after iron deficiency treatment. Tarm-92 variety of barley was exposed to the Fe deficiency for 5 days after grown on ½ Hoagland medium for 9 days. a. Root and shoots of plants after stress application. b. Leaf chlorosis after stress application. Bar: 1 cm.

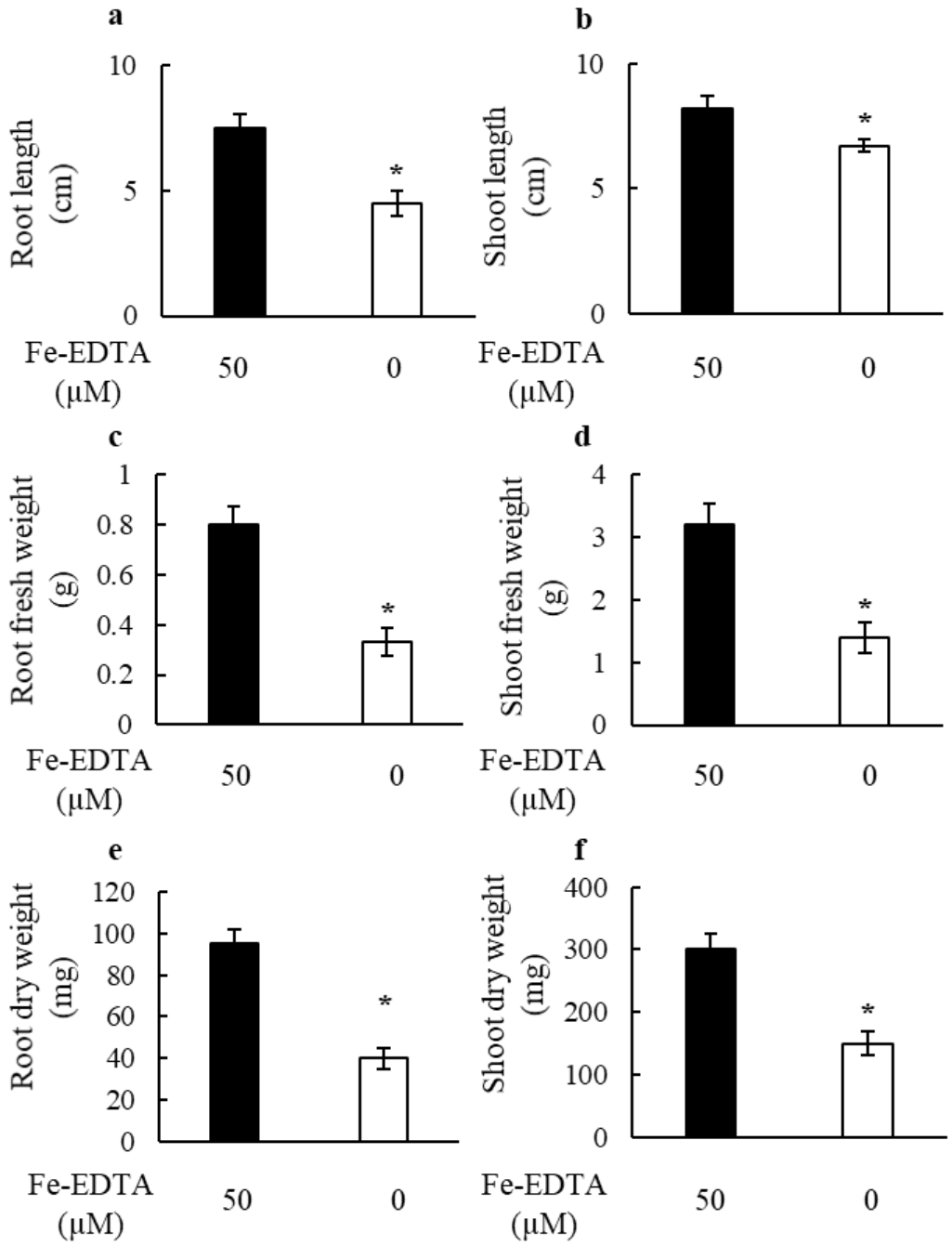

Figure 2. Physiological changes after Fe deficiency treatment. a. Root length. b. Shoot length. c. Root fresh weight. d. Shoot fresh weight. e. Root dry weight. f. Shoot dry weight. Values indicate the means ± SEM (n = 30 for an and b; n = 15 for c-f). * indicates a significant difference between the treatments according to Student's *t*-test ($P<0.05$).

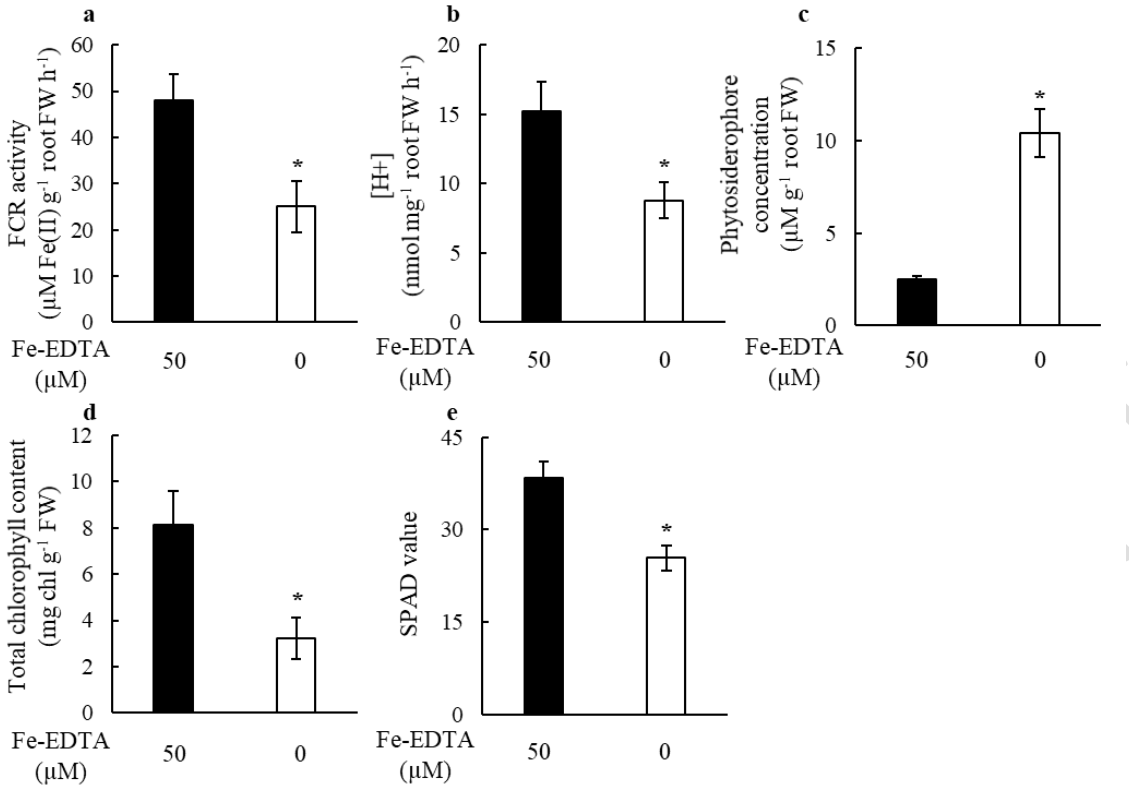

Figure 3. Biochemical changes after Fe deficiency treatment. a. FCR activity at the roots. b. Rhizosphere acidification. c. Phytosiderophore concentration. d. Total chlorophyll content. e. SPAD value. Values indicate the means ± SEM (n = 15). * indicates a significant difference between the treatments according to Student's *t*-test ($P<0.05$).

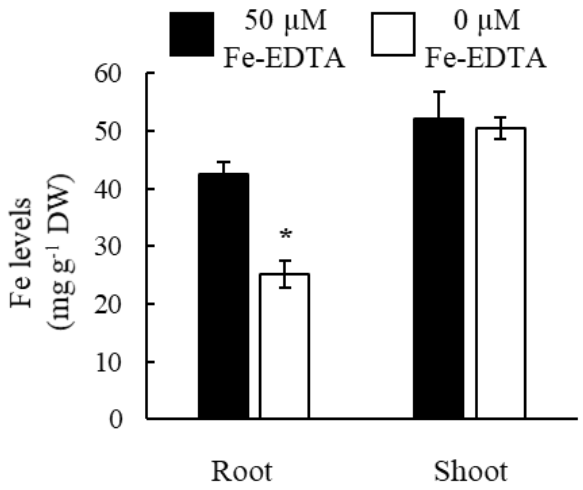

Figure 4. Fe levels in the roots and shoots after iron deficiency. Values indicate the means ± SEM (n = 3). * indicates a significant difference between the treatments according to Student's *t*-test ($P<0.05$).

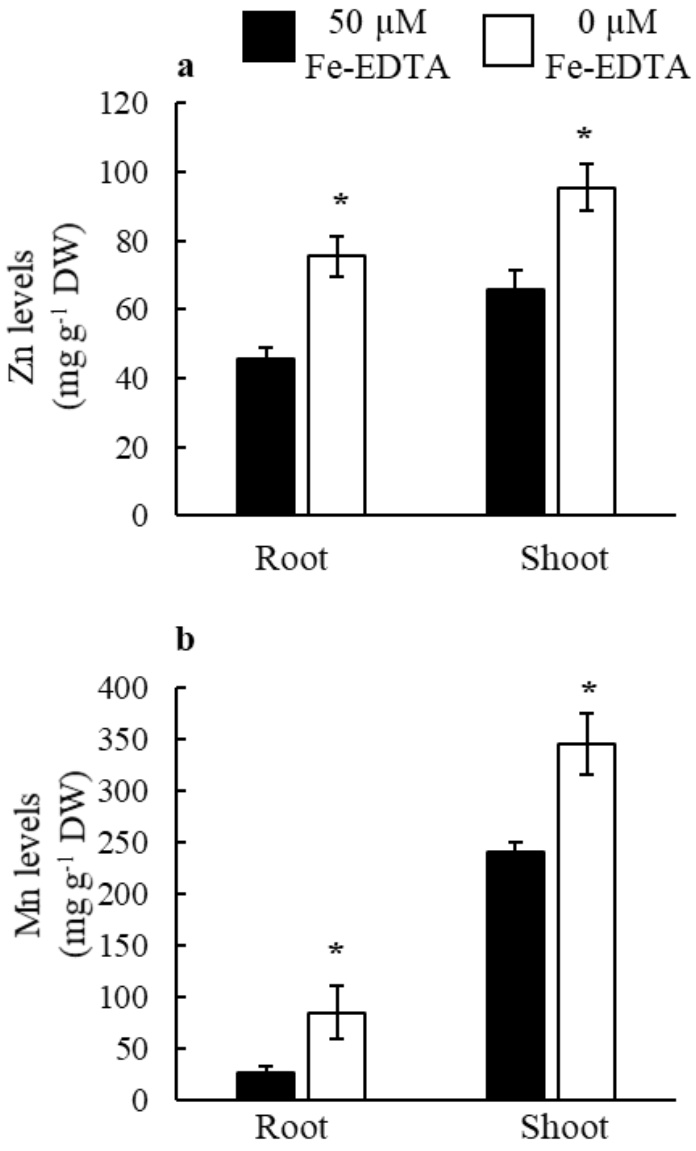

Figure 5. Zinc and manganese levels in the roots and shoots after iron deficiency. a. Zn levels. b. Mn levels. Values indicate the means ± SEM (n = 3). * indicates a significant difference between the treatments according to Student's *t*-test ($P<0.05$).

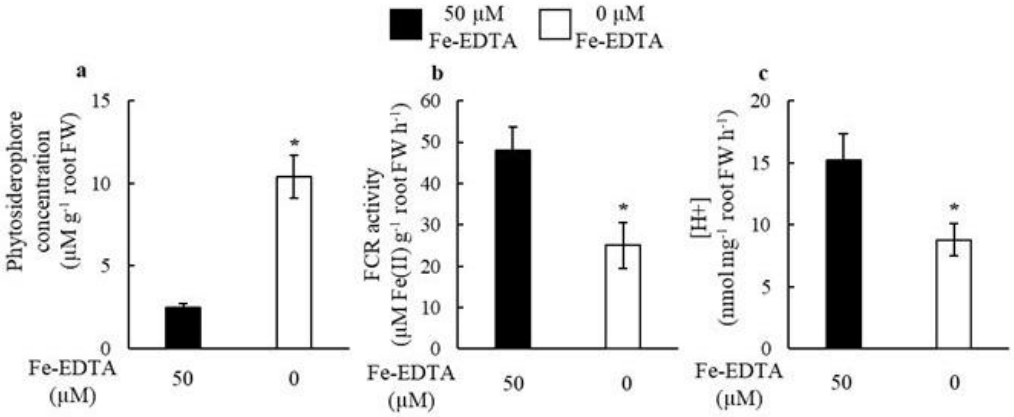

Figure 6. Biochemical changes in the roots after Fe deficiency. a. Phytosiderophore concentration. b. FCR activity at the roots. c. Rhizosphere acidification. Values indicate the means ± SEM (n = 15). * indicates a significant difference between the treatments according to Student's *t*-test ($P<0.05$).

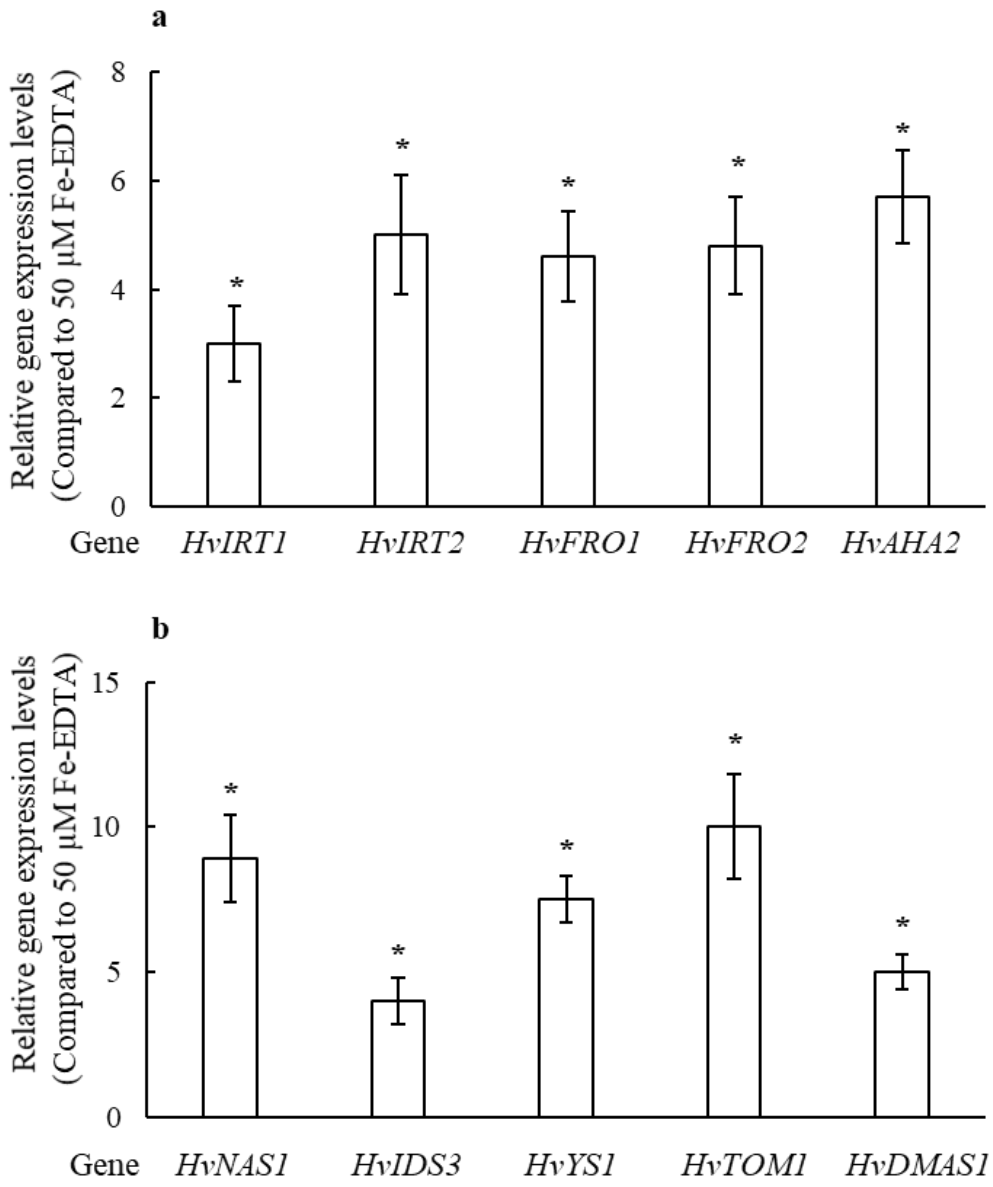

Figure 7. Relative expression of the genes in the roots of barley plants after Fe deficiency treatment. a. Genes involved in Strategy-I. b. Genes involved in Strategy-II. The expression level of each gene was compared to the expression level of the same gene in iron sufficient medium. Values indicate the means ± SEM (n = 3). * indicates a significant difference between the treatments according to Student's *t*-test ($P<0.05$).